Optimized Power Management Control Scheme for Transportation System Electrified with High Voltage DC Microgrid

N. Chaitanya*, Sumanth Yamparala**‡, K. Radharani***, P. Phani Prasanthi****

*Department of EEE, Associate Professor, R.V.R. & J.C. College of Engineering, Guntur-522019, India

**Department of EEE, Assistant Professor, R.V.R. & J.C. College of Engineering, Guntur-590019, India

***Department of EEE, Professor, R.V.R. & J.C. College of Engineering, Guntur-522019, India

****Department of Mechanical, Associate Professor, Prasad V. Potluri Siddhartha Institute of Technology, Vijayawada-520 007, India

(801chaitanya@gmail.com, sumanth46@gmail.com, korrapatiradharani@gmail.com, phaniprasanthi.parvathaneni@gmail.com)

‡Corresponding Author: Sumanth Yamparala, Department of EEE, R.V.R & J.C College of Engineering, Guntur, A.P, India, Tel: +91 9948198771, sumanth46@gmail.com

Received: 09.02.2022 Accepted: 19.03.2022

Abstract- Use of nonconventional energy sources for traction applications is a reliable solution to promote the green environment. Wind energy available is intermittent in nature. The usage of energy storage systems is essential for reliable operation. The Fuel cell and electrolyzer serve as backup sources for reliable operation, as do a super capacitor and a battery bank. Satisfactory performance of the PMDC motor can be achieved by operating at high voltages. The energy storage system is integrated with the grid by utilizing a DC-DC Bidirectional converter topology. A novel sliding mode current controller is proposed to balance the power within the operational constraints. This is the most promising controller among the different nonlinear current controllers due to the capability of direct calculation of required converter control voltage. Finally, plenary results are obtained through simulation. The suggested control scheme's real-time performance is evaluated using a hardware test bench setup using a SPARTAN 6 FPGA kit.

Keywords Sliding mode controller, DC Microgrid, Bidirectional DC-DC converter, Kalman filter, MATLAB (Matrix Laboratory), Simulink.

NOMENCLATURE

P_{wind}	Instantaneous output power.
$P_{Supercapacitor}$	Total value of power supplied/absorbed by super capacitor.
P_{Load}	Immediate power consumed by the load
$P_{Battery}$	Total value of power supplied/absorbed by Battery
Q	Process noise covariance
$U_{g\alpha\beta}$, $V_{g\alpha\beta}$	Grid and converter voltage vectors
$I_{g\alpha\beta}$	Line current
R_g, L_g	Line resistance and inductance
P_g, Q_g	Real and reactive powers
SMCC	Sliding mode current controller
SESS	Smart energy storage system
MPPT	Maximum power point technique

1. Introduction

Now a days, everyone looks after DC Microgrid due to its flexibility and efficiency. According to the daily load variations of residential localities, a mathematical model is presented by considering the data and discussing the importance of system efficiency in [22]. Efficiency, multi-stage power electronic converters, and complex frequency and regulation problems are the primary motivators for shifting the focus from AC Microgrid to DC Microgrid.[1] [10] [20-21]. Energy management of DC Microgrid with decoupling, state machine and fuzzy logic strategies was discussed to validate the PI control strategy, and concluded that PI control strategy is better than decoupling and state

machine control strategies in terms of hydrogen consumption, Fuzzy controller performance is close to PI, as discussed in [24]. To meet the needs of business and society, scientists have been encouraged to use non conventional energy sources to reduce transmission and distribution losses [11]-[13]. Wind generation is the most promising generation according to the Indian environment, but the sporadic nature of this source arises due to changes in levels of temperature. Hence it is better to adopt an efficient MPPT technique like [25] the Kalman Maximum power point algorithm. The Neural network based kalaman filter [23] is designed to improve the accuracy of electrical parameters and verify the performance of MPPT using the perturb and observe algorithm, kalman filter, under different irradiance and temperature levels, and it was concluded that the kalman filter is able to track maximum power better than P&O algorithm. In references [2][3], they also performed the experimental evaluation of different MPPT algorithms and concluded that Kalman filter MPPT algorithm gives better results when compared to remaining MPPT Techniques. Because of the promising nature, such as increasing overall capacity, handling of sporadic nature, transmission relief, and good quality, storage systems are very important in DC Microgrids for energy backup. Energy storage systems are subdivided into transient nature like super capacitors and relaxed nature devices like batteries. Super capacitors, also known as electric double layer capacitors, are high capacitance capacitors with numerous advantages, such as long life, good power density, and an extraordinary temperature range. Although the super capacitor provides greater performance in most areas, it cannot be employed as the primary ESS due to its low energy density. Similarly, super capacitor technology is still developing, so they are not as trustworthy as traditional batteries. In a hybrid energy storage system, batteries and super capacitors can complement each other. In [26], they proposed a DC microgrid with PV, a Fuel Cell, and a hybrid energy storage system including a super capacitor and a lithium-ion battery for better improvement of power quality in ESS. [14] investigates a dq power flow based storage unit controller for microgrids, ensuring load balancing in grid connected and disconnected modes, as well as under unbalanced load conditions. Generally, the electrolyzer tapped additional power at the common bus bar. A Fuel cell and an electrolyzer work together to provide a smart energy storage system (SESS) [15]. DC-DC power conversion circuits face issues like efficiency and stress at very high operating voltages. In this paper, the DC-DC converter uses inductors which are coupled in an interleaved manner. High gain input and parallel output series DC-DC converter intended for boosting purpose is presented in [5][19]. Traditional DC-DC converters failed to achieve low level terminal voltage to high level terminal voltage conversions to grab the advantages like high gain, bringing down the complexity of controlling a bidirectional circuit with novel multistage non isolated three port converter to feed residential load applications. Due to increased number of ports, this system is flexible to change the rate of PV panels and even it is possible to add more batteries [6]. BLDC driven Electric braking methods at all speeds with different number of switches are proposed in [4]. By considering all advantages and methods of the above references, this work presents control of wind based power generation with DC Microgrid added by a super capacitor and a Battery. The sizing of charge controller for batteries which are suitable as a backup source for wind power plants is discussed in [7]. For smart energy storage systems, fuel cells are also added to maintain proper DC bus voltage. After selection of components or sources for the microgrid, need to focus on power management methodology. One of the popular methodologies is outer PI voltage control and an inner current controller for switching pulse generation. But these types of controllers fail due to large settling times because of large overshoots and also because of continuing steady state errors that deviate the system output from the desired output. To relieve all the above consequences, it is decided to apply an outer loop voltage controller in addition to a nonlinear type of current controller such as a sliding mode current controller. The Conventional sliding mode controller leads to long term convergent behavior due to mismatches in estimation of system uncertainty bounds. There will be sustainable steady state error discussed in [9]. A sliding mode controller based on a decentralized architecture is proposed for the stability of DC microgrids [27]. The sliding mode controller is the solution to maintain stable DC bus voltage because DC bus voltage will become unstable due to constant power load as discussed in [16][18] and the necessity of sliding mode controller for power electronic converters in [17]. The main goal of DC Microgrid is the stability of DC bus voltage. This paper concentrated on the stability of DC Microgrids by varying the speed of wind. According to the references above, it is observed that the kalman MPPT algorithm is better at tracking the maximum power available from wind turbines. A new kind of sliding mode current controller is proposed to make the system free from dynamic swings, to settle the system output stable in a short time, and to keep the large overshoots away.

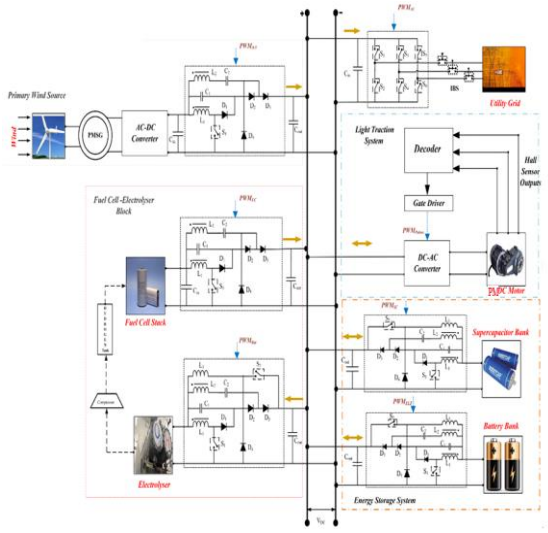

Fig. 1. Wind source based DC microgrid under study

The PMDC motor is operated both in motoring mode and regenerative mode under different load torque conditions to observed stable DC bus parameters. Overall , the designed DC Microgrid is stable and able to balance the load under different operating conditions. The proposed controller configuration for DC Microgrid is tested using MATLAB/Simulink and plenary outcomes are obtained, and the results are compared with the traditional controller, which is an outer PI loop controller with an inner PWM current controller.

2. System Under Consideration

In this paper, Wind Power plant is used as the main source. Fuel Cell, Super Capacitors and Battery is used as the holdup sources for electric traction applications. The system under consideration is shown in Fig.1. A Kalman filter based MPPT technique [8] is applied to the wind power plant to extract the maximum output. In this high gain DC-DC converter, voltages are applied to attain high terminal voltages. Here, for the actual division of power among all the DC microgrids, the sliding mode current controller power management technique is applied. To identify the effectiveness of the controller, the designed system is tested under MATLAB/Simulink environment.

The output power balance equation is

$$P_{WIND/Fuelcell} = P_{Supercapacitor} + P_{Battery} + P_{Load} \quad (1)$$

Where $P_{WIND/Fuelcell}$ is the instantaneous output power generated by wind power plant or fuel cell.

$P_{Supercapacitor}$ is the total value of power flowing from or obtaining to the super capacitor.

$P_{Battery}$ is the total value of power flowing from or obtaining to the battery while charging and discharging.

P_{Load} is considered as immediate power consumed by the load.

3. Power Management Control Strategy

3.1 Control of DC-DC Converter

In this case, the boost converter switching pulses are generated by the Kalman MPPT technique [9]. To model the system and to generate switching pulses for the boost converter circuit, the system is modelled using state space analysis [8].

The state of a system is represented by

$$X[x+1] = A\,X[x] + B\,U[x] + C\,Z[x] \quad (2)$$

$$Y(x) = DX[x] + U[x] \quad (3)$$

Where X[x] represents state, U[x] represented as input, Y[x] is represented as output, Z[x] is considered as process noise and U[x] represents noise of measurement.

Under noisy conditions, this Kalman MPPT algorithm shows its effectiveness while measuring the state of a considered network.

This MPPT algorithm is implemented by employing recursive assessment updates and temporal updates across time to fix the state estimations.

To evaluate the actual values of time and assessment corrections, need is there to include the assessment update of the Kalman gain

$$K[x] = M[x]-(M[x]- +V)- \quad (4)$$

V is the assessment noise covariance (Correction value).

M[x]- is the covariance of the error from the most recent time interval. The error in gain updates the estimates of U[x].

$$\hat{U}[X] = \hat{U}[X]^{-} + K[X][Y(X) - \hat{U}[X]^{-}) \quad (5)$$

Updates of error covariance M[x]=(1-K[x]) M[x]-

Time update (predicted value)

$$\hat{U}[X+1]^{-} = \hat{U}[X] + N.\frac{Q[X] - Q[X-1]}{U[X] - U[X-1]} \quad (6)$$

N is the specific step size

$M[x+1]^{-}=M[x]+Q$, Q is the process noise covariance. With all these measurement and time updates, the results are near to the maximum power point.

3.2 Designing of Current Controller for Grid Connected Voltage Source Converter

3.2.1 *Practices of VSC Coupled to The Grid*

In a fixed frame of reference assume both VSC and grid are ideal voltage sources. The supply, converter voltages, and line currents have the following relationship [8] :

$$U_{g\alpha\beta} = I_{g\alpha\beta}R_g + L_g\,\frac{dI_{g\alpha\beta}}{dt} + V_{g\alpha\beta} \quad (7)$$

The grid-side instantaneous real and reactive power values may be computed as

$$P_g + jQ_g = -\frac{3}{2} U_{g\alpha\beta} * \hat{I}_{g\alpha\beta} \quad (8)$$

$$P_g = -\frac{3}{2}(U_{g\alpha} i_{g\alpha} + U_{g\beta} i_{g\beta}) \quad (9)$$

$$Q_g = -\frac{3}{2}(U_{g\beta} i_{g\alpha} - U_{g\alpha} i_{g\beta}) \quad (10)$$

From equations (9) & (10) igα ,igβ (line currents) represented as

$$\begin{bmatrix} i_{g\alpha} \\ i_{g\beta} \end{bmatrix} = \frac{2}{3U_g^2} \begin{bmatrix} -u_{g\alpha} & -u_{g\beta} \\ -u_{g\beta} & u_{g\alpha} \end{bmatrix} \begin{bmatrix} P_g \\ Q_g \end{bmatrix} \quad (11)$$

$$U_g = \sqrt{u_{g\alpha}^2 + u_{g\beta}^2}$$

3.2.2 *Proposed Current Controller*

The proposed control method is established according to the creation of an intermittent control signal that steers the operating states of the system regarding the particular manifolds in the state space. These manifolds are chosen in such a way that the control system exhibits the desired behavior when the states converge on them. In this work, The stationary-frame line currents of grid-connected VSCs are regulated using a sliding mode current control (SMCC) system [23].

3.2.2.1 Sliding Surface:

The sliding surface is configured as [9]

$$S = \begin{bmatrix} S_\alpha & S_\beta \end{bmatrix}^T \quad (12)$$

The switching surfaces play a crucial role, which are built using back-stepping and nonlinear damping approaches [23].

$$S_\alpha = e_\alpha(t) + K_\alpha \int_0^t e_\alpha(\tau) d\tau - e_\alpha(0) \quad (13)$$

$$S_\beta = e_\beta(t) + K_\beta \int_0^t e_\beta(\tau) d\tau - e_\beta(0) \quad (14)$$

Where,

$e_\alpha(t) = i_{g_\alpha}^* - i_{g\alpha}$, $e_\beta(t) = i_{g\beta}^* - i_{g\beta}$

Approximate errors are $e_\alpha(t)$, $e_\beta(t)$. K_α & K_β are gains.

When the system states reach the sliding manifold and slide down the surface, the process is said to be complete.

$$S_\alpha = S_\beta = \frac{dS_\alpha}{dt} = \frac{dS_\beta}{dt} = 0 \quad (15)$$

From (13) & (14)

$$\frac{de_\alpha(t)}{dt} = -K_\alpha e_\alpha(t) \quad (16)$$

$$\frac{de_\beta(t)}{dt} = -K_\beta e_\beta(t) \quad (17)$$

The above two error equations ensure that the power errors are converges to zero.

Here Kα & Kβ are positive values chosen for desired transients of the system.

3.2.2.2 Sliding Mode Current Control (SMCC) Law

The aim of the SMCC design is to compel the system state trajectory to interact with the surfaces of the switching stated above. The SMCC [17] system was devised in this study to create the inverter's reference voltage as the input to the SVM module.

By differentiating Sα and Sβ in (13)& (14)

$$\frac{dS_\alpha}{dt} = \frac{de_\alpha}{dt} + K_\alpha e_\alpha(t) = \frac{d}{dt}(i_{g\alpha}^* - i_{g\alpha}) + K_\alpha(i_{g\alpha}^* - i_{g\alpha}) \quad (18)$$

$$\frac{dS_\beta}{dt} = \frac{de_\beta}{dt} + K_\beta e_\beta(t) = \frac{d}{dt}(i_{g_\beta}^* - i_{g_\beta}) + K_\beta(i_{g_\beta}^* - i_{g_\beta}) \quad (19)$$

From (11), the reference currents can be obtained as

$$\begin{bmatrix} i_{g\alpha}^* \\ i_{g\beta}^* \end{bmatrix} = \frac{2}{3U_g^2} \begin{bmatrix} -u_{g\alpha} & -u_{g\beta} \\ -u_{g\beta} & -u_{g\alpha} \end{bmatrix} \begin{bmatrix} P_g^* \\ Q_g^* \end{bmatrix} \quad (20)$$

where P_g^* & Q_g^* are the immediate real and reactive power reference values, respectively.

$$\frac{d}{dt}\begin{bmatrix} i_{g\alpha}^* \\ i_{g\beta}^* \end{bmatrix} = \frac{2}{3U_g^2} \begin{bmatrix} -\frac{d}{dt}u_{g\alpha} & -\frac{d}{dt}u_{g\beta} \\ -\frac{d}{dt}u_{g\beta} & -\frac{d}{dt}u_{g\alpha} \end{bmatrix} \begin{bmatrix} P_g^* \\ Q_g^* \end{bmatrix} \quad (21)$$

Consider a grid voltage that isn't distorted,

$$u_{g\alpha} = U_g \sin(\omega_1 t)$$

$$u_{g\beta} = -U_g \cos(\omega_1 t)$$

As a result, the instant grid voltage variations are calculated as follows:

$$\frac{du_{g\alpha}}{dt} = \omega_1 U_g \cos(\omega_1 t) = -\omega_1 u_{g\beta} \tag{22}$$

$$\frac{du_{g\beta}}{dt} = \omega_1 U_g \sin(\omega_1 t) = \omega_1 u_{g\alpha} \tag{23}$$

$$\frac{d}{dt}\begin{bmatrix} i_{g\alpha}^* \\ i_{g\beta}^* \end{bmatrix} = \frac{2\omega_1}{3U_g^2}\begin{bmatrix} u_{g\beta} & -u_{g\alpha} \\ -u_{g\alpha} & -u_{g\beta} \end{bmatrix}\begin{bmatrix} P_g^* \\ Q_g^* \end{bmatrix} \tag{24}$$

The line currents' derivative is written as

$$\frac{d}{dt}\begin{bmatrix} i_{g\alpha} \\ i_{g\beta} \end{bmatrix} = \frac{1}{L_g}\begin{bmatrix} u_{g\alpha} & -v_{g\alpha} \\ u_{g\beta} & -v_{g\beta} \end{bmatrix} - \frac{R_g}{L_g}\begin{bmatrix} i_{g\alpha} \\ i_{g\beta} \end{bmatrix} \tag{25}$$

$\frac{dS}{dt} = F + \frac{1}{L_g} V_g$ Where

$$F = \begin{bmatrix} F_\alpha & F_\beta \end{bmatrix}^T, \quad V_g = \begin{bmatrix} V_{g\alpha} & V_{g\beta} \end{bmatrix}^T$$

$$\begin{bmatrix} F_\alpha \\ F_\beta \end{bmatrix} = \frac{2\omega_1}{3U_g^2}\begin{bmatrix} u_{g\beta} & -u_{g\alpha} \\ -u_{g\alpha} & -u_{g\beta} \end{bmatrix}\begin{bmatrix} P_g^* \\ Q_g^* \end{bmatrix} - \frac{1}{L_g}\begin{bmatrix} u_{g\alpha} & -R_g i_{g\alpha} \\ u_{g\beta} & -R_g i_{g\beta} \end{bmatrix} + \begin{bmatrix} K_\alpha (i_{g\alpha}^* - i_{g\alpha}) \\ K_\beta (i_{g\beta}^* - i_{g\beta}) \end{bmatrix} \tag{26}$$

A Lyapunov technique is commonly employed in sliding mode control design to identify the context of the control law that will push the equilibrium manifold's state orbit. It is decided to use the quadratic Lyapunov function.

$$W = \frac{1}{2} S^T S \geq 0 \tag{27}$$

The differentiation of W on the state trajectories of (27) is given by

$$\frac{dW}{dt} = \frac{1}{2}\left(S^T \frac{dS}{dt} + S\frac{dS^T}{dt}\right) = S^T \frac{dS}{dt} = F + \frac{1}{L_g} V_g \tag{28}$$

The switch control law must be designed in such a way that the time derivative of W is clearly negative with 'S' not equal to zero. As a result, the following control law has been chosen:

$$V_g = -L_g \left\{ \begin{bmatrix} F_\alpha \\ F_\beta \end{bmatrix} + \begin{bmatrix} K_{\alpha 1} & 0 \\ 0 & K_{\beta 1} \end{bmatrix}\begin{bmatrix} sign(S_\alpha) \\ sign(S_\beta) \end{bmatrix} \right\} \tag{29}$$

where $K_{\alpha 1}$ & $K_{\beta 1}$ are +ve control gains, $sign(S_\alpha)$ & $sign(S_\beta)$ are switching pulses for the line currents.

3.2.2.3 *The Proof of the Stability*

For stability make $\frac{dW}{dt} < 0$ .If $S_\alpha \cdot sign(S_\alpha) > 0$ & $S_\beta \cdot sign(S_\beta) > 0$ then

$$\frac{dW}{dt} = S^T \frac{dS}{dt} = -S^T \begin{bmatrix} K_{\alpha 1} & 0 \\ 0 & K_{\beta 1} \end{bmatrix}\begin{bmatrix} sign(S_\alpha) \\ sign(S_\beta) \end{bmatrix} \tag{30}$$

The differentiation of Lyapunov function $\frac{dW}{dt}$ is certainly negative so that it achieves asymptotically steady behavior.

3.2.2.4 *Demonstration of Robustness*

$$\frac{dS}{dt} = F + \frac{1}{L_g} V_g + H$$

'S' is the sliding surface

$H = \begin{bmatrix} H_\alpha & H_\beta \end{bmatrix}^T$, H represents disturbances of the system.

Eq (30) can be written as

$$\frac{dW}{dt} = S^T \frac{dS}{dt} = -S^T \left\{ \begin{bmatrix} H_\alpha \\ H_\beta \end{bmatrix} - \begin{bmatrix} K_{\alpha 1} & 0 \\ 0 & K_{\beta 1} \end{bmatrix}\begin{bmatrix} sign(S_\alpha) \\ sign(S_\beta) \end{bmatrix} \right\} \tag{31}$$

If $K_{\alpha 1} > |H_\alpha|$ & $K_{\beta 1} > |H_\beta|$, The Lyapunov function differentiation is still clearly negative. As a result, the SMCC has a high level of robustness.

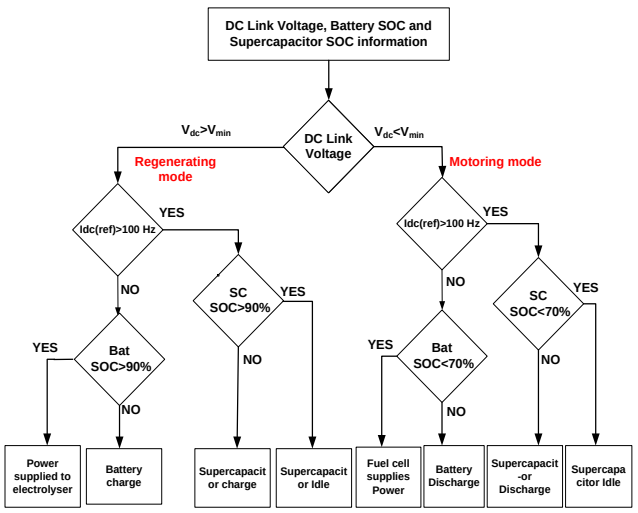

Fig. 2. Flow chart for the Power flow control

4. Simulation Results And Discussion

The Wind power system connected to grid as displayed in Fig.1 has been designed and evaluated on the MATLAB/SIMULINK software platform under various test cases. Fig. 2 shows the flowchart for power flow control.

Case 1: The motor's load torque is constant in this example, at 3.5 Nm. From 0 to 1s, the speed of the wind remains constant at 12 m/s, then gradually decreases to 9 m/s from 1s to 4s. Finally, from 4s to 5s, the speed is prolonged at 9 m/s. The SOC of a battery is defined as less than 70%.

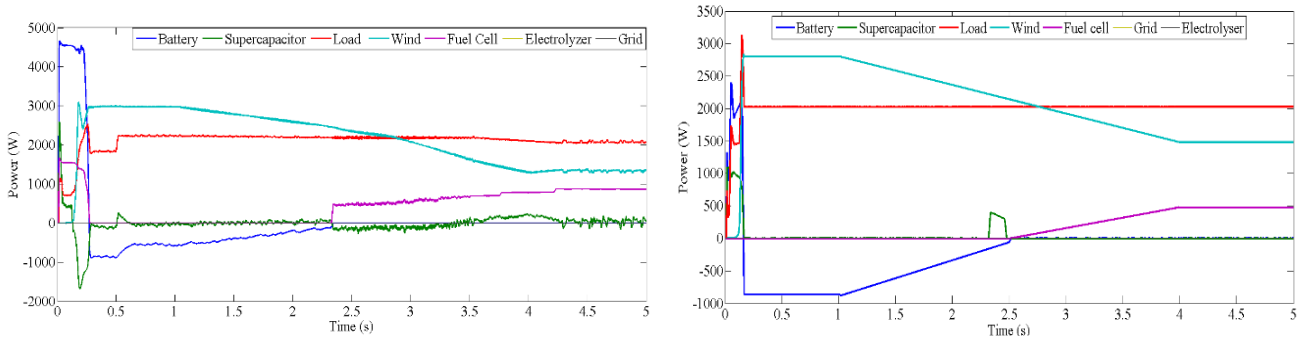

Fig. 3. Participants in the microgrid sharing power

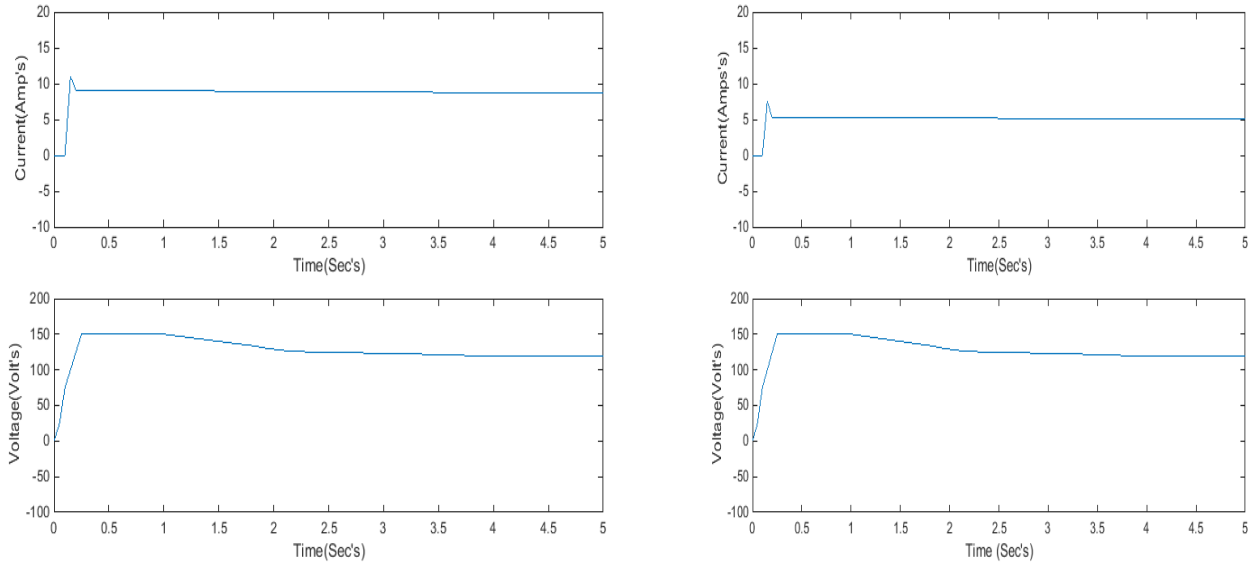

Fig. 4. Wind turbine parameters of the boost converter (a) current (b) voltage

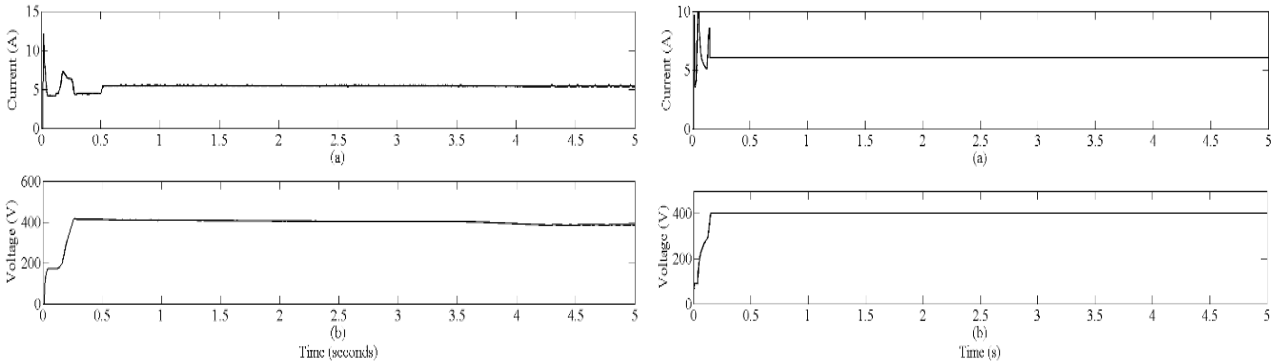

Fig.5. DC bus parameters (a) Current (b) Voltage

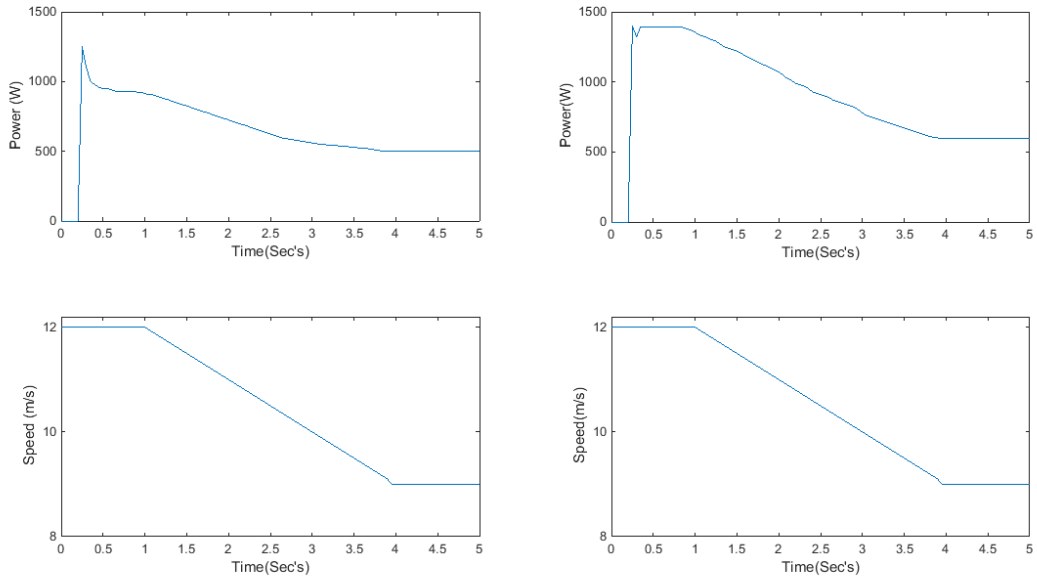

Fig. 6. Parameters of wind turbine (a) wind plant output (b) Speed of the wind

Case 2: The wind system speed is kept constant at 12 m/s in this scenario. The PMDC motor is in motoring mode. From 0 to 1.5s, the load torque is kept constant at 5 Nm. At 1.5 Sec, the torque abruptly increasing to 6 Nm . Finally, at 3.5s, it is expanded to 8 Nm and maintained at 5s. The battery's state of charge (SOC) is greater than 90%.

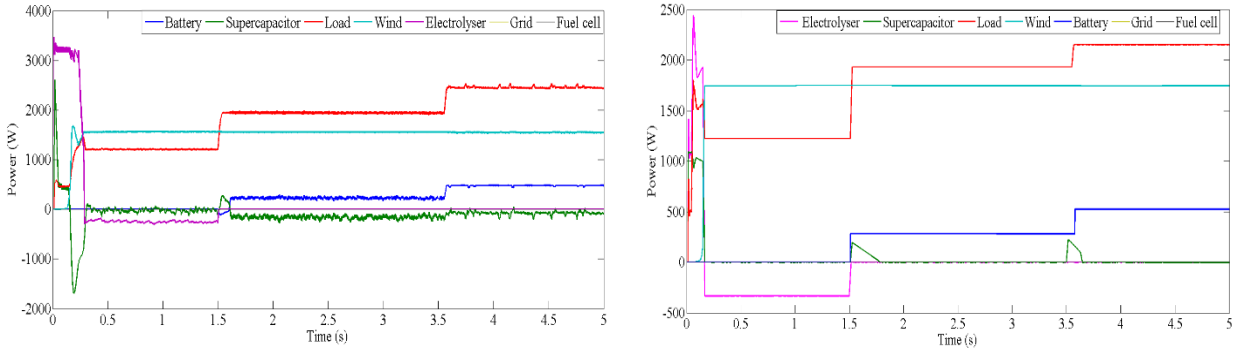

Fig. 7. Participants in the microgrid share power.

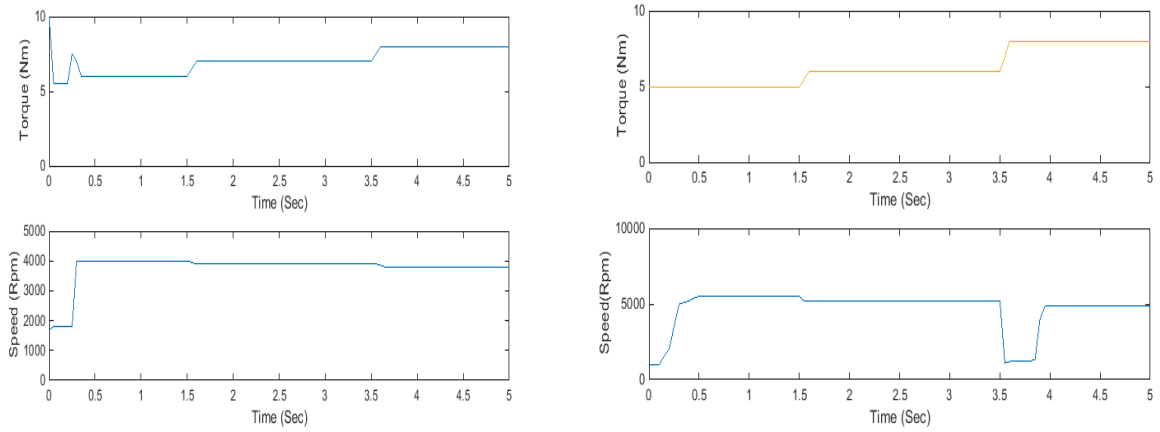

Fig. 8. Parameters of PMDC motor (a) Torque (b) Speed

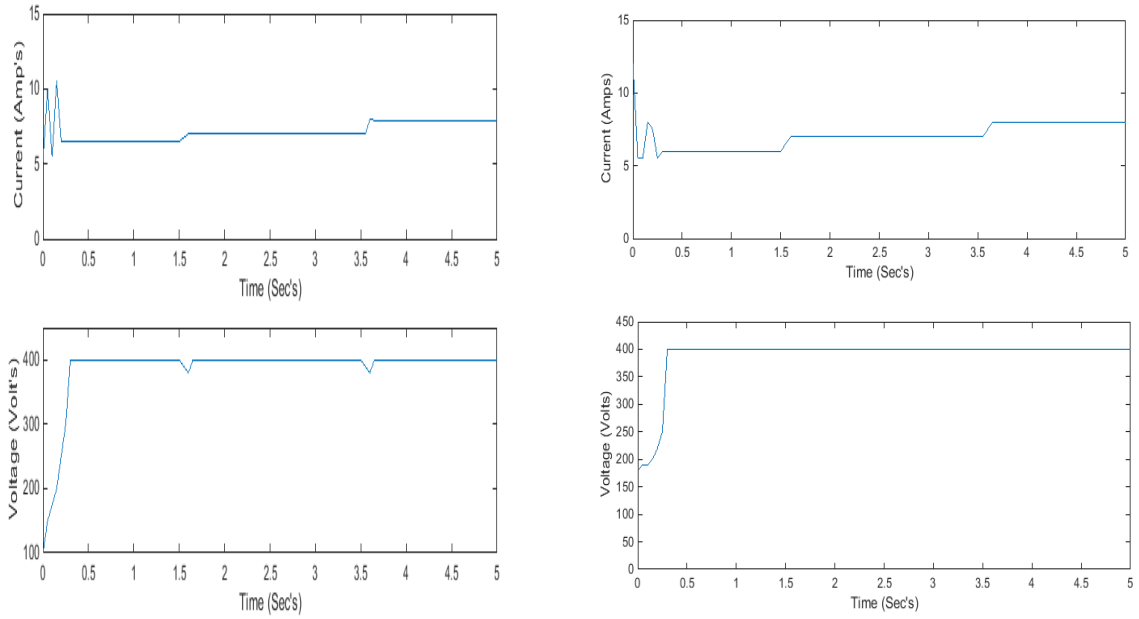

Fig. 9. Parameters of DC bus (a) current (b) voltage

Case 3: The wind speed is kept constant in this case, at 12 m/s. The PMDC motor is in regenerative mode. From 0 to 1.5s, the load torque is maintained at 1 Nm, then it is immediately dropped to -0.5 Nm at 1.5s. Finally, at 3.5s, it drops to -1 Nm and stays there until 5s. The battery's state of charge (SOC) is less than 70%.

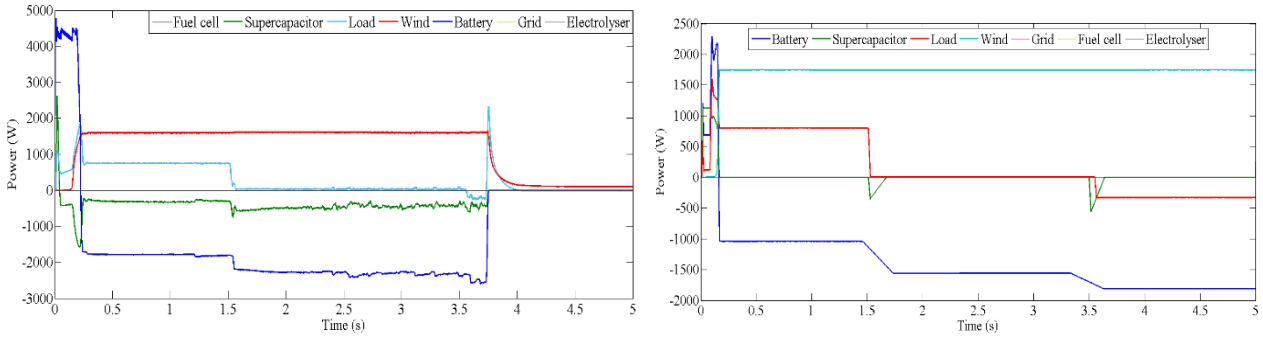

Fig. 10. Participants in the microgrid sharing power.

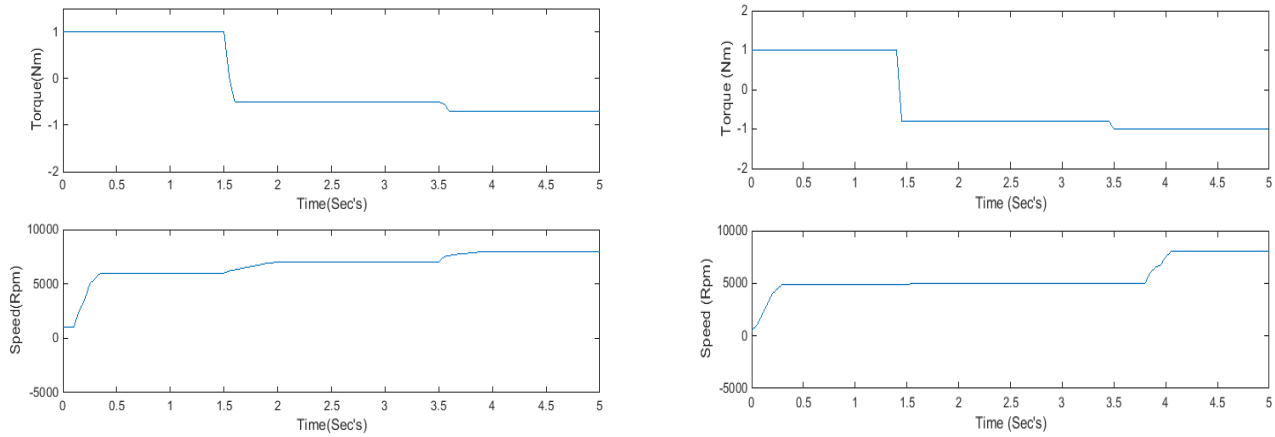

Fig. 11. Parameters of PMDC motor (a) Torque (b) Speed

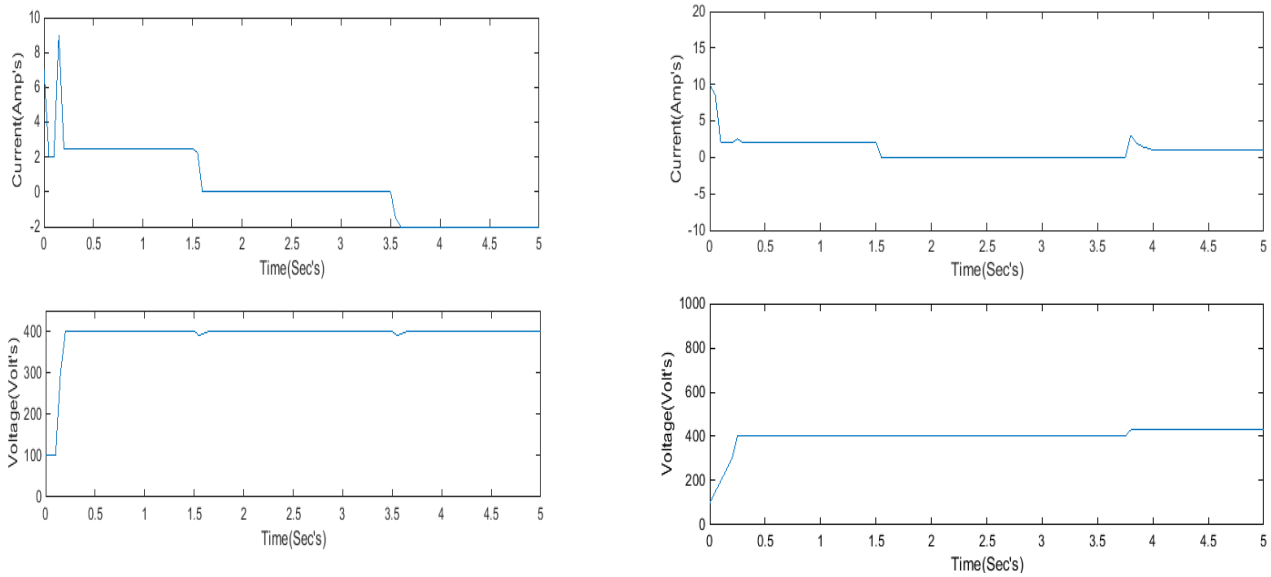

Fig. 12. Parameters of DC bus (a) current (b) voltage

The results obtained using the existing power management controller are shown in Fig. 3 – 12 (left side) (i.e., outer PI loop, inner PWM current controller). The results of the proposed sliding mode based power management algorithm are shown in Figures 3–12 (right side). The output waveforms from the 3-phase rectifier are shown in Fig. 4 and are fed into the high-gain boost converter. The DC common bus bar specifications are shown in Figure 5. In comparison to the existing controller, the proposed controller produces better results (see Figs. 4 and 5). Because the wind turbine's high-gain DC-DC boost converter uses the Kalman algorithm, it produces higher output power for a given speed than a traditional MPPT, as illustrated in Fig. 6. With the motoring mode, Fig. 7 depicts the power-sharing among microgrid participants (i.e., Case 2). When the battery's state of charge (SOC) is more than 90%, battery stops charging since the torque of the load is lesser than the output power. As shown in Fig. 7, the electrolyzer receives up to 1.5 seconds of power before the battery supplies the necessary power for the load. Even under fluctuating load torque settings, the suggested controller is assured to produce good results, as shown in Fig.7. The torque characteristics, speed characteristics of the PMDC motor are shown in Fig.8. With the controller which is mentioned in literature, the speed is disrupted at 3.5s due to the abrupt rise in load torque, but with the proposed controller, the speed is in a consistent manner.

The DC bus bar parameters are shown in Fig.9. The DC bus voltage with the suggested controller has smaller overshoot and is steadier. The power-sharing among microgrid participants with the regenerative mode is depicted in Fig. 10. (i.e., Case 3). As shown in Fig. 10, The proposed controller, which is utilized to manage the power, produces better results throughout the regenerating time, as compared to the controller mentioned in the literature, which failed to maintain stability. Figure 11 exhibits the PMDC motor's torque and speed characteristics. The controller mentioned in the literature accounts for the sudden increase in load torque, but with the proposed controller, the speed remains constant. The suggested controller is able to maintain DC bus bar voltage constant. Finally, when compared to the existing power management controller, the suggested controller has a faster settling time, a lower transient response, and the intended output is produced without deviances. DC bus parameters are shown in Fig. 12.

Hardware Analysis:

The DC Microgrid test setup has evolved to inspect the sliding mode current controller. The test setup consists of wind generation, battery- super capacitor, PMDC motor, sensor circuits, and a SPARTAN 6 FPGA board. The wind plant is implemented using an uneven DC source. The rating of the battery is 12v, 7 Ah and a capacitor bank of 10 mF is taken. The experimental test setup is shown in Fig.13.

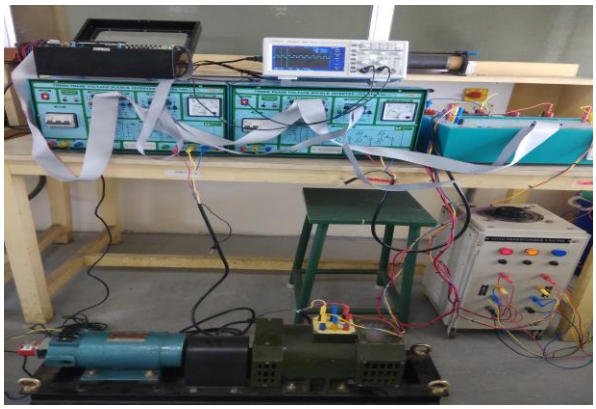

Fig.13. Experimental Test setup

The test setup is run with a constant load torque of 2 Nm. The voltage and current waveforms that arise are depicted in Fig. 14. The analysis is also carried out with two load torques (i.e., 1 Nm and 2 Nm), the accompanying voltage and current waveforms given in Fig. 15. It has been confirmed that the suggested controller, which generates DC-DC converter pulses based on the load as indicated in Fig. 16, maintains a steady load voltage at all times.

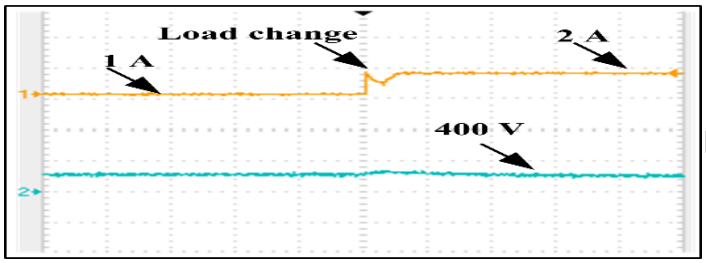

Fig. 14. Voltage and Current waveforms at a load torque of 1Nm & 2 Nm. (Orange line: Y- (current): 1 Amps/div; X(Time): 0.5secs /div; Blue line : Y- (voltage): 300 Volts/div; X-(time): 0.5secs /div))

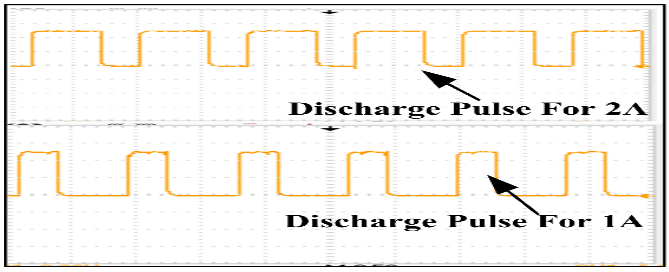

Fig. 15. Switching pulses supplied to DC-DC converter (SCALE: Y- axis: 1Volts/div; X-axis: 0.5micro sec/div)

5. Conclusion

The generation of power should be expanded in tandem with the maintenance of clean and environmentally friendly sources, as the demand for electricity is rapidly increasing. In this situation, this study proposes a strategy for generating clean energy from wind sources as well as energy storage devices in order to ensure grid stability for traction applications. This study describes the design, analysis, and implementation of a dynamic power management scheme with a sliding mode controller for a DC microgrid system that includes a wind generator, energy storage system, and smart energy storage system. By ensuring equitable power distribution among microgrid participants, the controller utilized in this system maintains a persistent voltage at the DC- bus bar in a variety of circumstances. MATLAB/SIMULINK is used to model the entire system, and the DC Microgrid is tested in a real time environment. Both simulation and real-time results are satisfactory, demonstrating the effectiveness of power sharing.

References

[1] Jingfeng Mao, Xiaotong Zhang, Tengfei Dai, Aihua Wu and Chunyun Yin, “An Adaptive Backstepping Sliding Mode Cascade-Control Method for a DC Microgrid Based on Nonlinear Virtual Inertia”, Electronics 2021, 10, 3100, pg.no :1-21.

[2] Dr. Y. Beck, N. Sober, “Experimental Verification and Comparative Study of Various MPPT Algorithms”, Automatika Journal for Control, Measurement, Electronics, Computing and Communications, Vol.57, No.2, 2016.

[3] Ricco M, Manganiello P, Monmasson E, G. Petrone G and G. Spagnuolo G. “FPGA-Based Implementation of Dual Kalman Filter for PV MPPT Applications”. IEEE Trans. Industrial Informatics 2017; 13(1): 176-185

[4] A. Joseph Godfrey, V.Sankaranarayanan, “A new electric braking system with energy regeneration for a BLDC motor driven electric vehicle”,Engineering Science and Technology, an international journal 21 (2018): 704-713.

[5] Farhan Mumtaz, Nor Zaihar Yahaya, Sheikh Tanzim Meraj, Balbir Singh, Ramani Kannan, Oladimeji Ibrahim, “Review on non-isolated DC-DC converters and their control techniques for renewable energy applications”, Ain Shams Engineering Journal 12 (2021) 3747-3763.

[6] Abdelsalam Elmakawi, Kamil Bayindir, “ A High-Gain Non-Isolated Three-Port Converter for Building-Integrated PV Systems”, Electronics 2022,11,387.

[7] Yazdi, Mohammadreza S., Sholeh B. Karkani, and Ercan Erturk. "Sizing of an Islanded Wind Solar Battery Hybrid Power System for a Zero-Energy House in Afyon Turkey." International Journal of Renewable Energy Research (IJRER) 11.3 (2021).

[8] V. Narendra Kumar, Narendra Babu P , R. Kiranmayi, PierluigiSiano, “Improved Power Quality in a Solar PV Plant Integrated Utility Grid by Employing a Novel Adaptive Current Regulator”, IEEE SYSTEMS JOURNAL, VOL. 14, NO. 3,4308-4319, SEPTEMBER 2020.

[9] En-Chih Chang, “Study and Application of Intelligent Sliding Mode Control for Voltage Source Inverters”, Energies 2018,11,2544.

[10] Adam Hirsch, Yael Parag, Josep Guerrero, “ Microgrids : A review of technologies, key drivers and outstanding issues" Renewable and Sustainable Energy Reviews 90 (2018) 402-411.

[11] Akeyo, O.M.; Patrick, A.; Ionel, D.M. “Study of Renewable Energy Penetration on a Benchmark Generation and Transmission System”. Energies 2021, 14, 169.

[12] Ahmed, D.; Ebeed, M.; Ali, A.; Alghamdi, A.S.; Kamel, S. “Multi-objective energy management of a micro-grid

considering stochastic nature of load and renewable energy resources". Electronics 2021, 10, 403.

[13] Ma, J.; Zhang, S.; Li, X.; Du, D. "Integrating base-load cycling capacity margin in generation capacity planning of power systems with high share of renewable". Trans. Inst. Meas. Control. 2019, 42, 31–41.

[14] R.Ahshan, S.A.Saleh and Abdullah Al-Badi, "Performance Analysis of a Dq Power Flow-Based Energy Storage Control System for Microgrid Applications", IEEE Access 2020, Volume:8 ,PP. 178706- 178721.

[15] Veniamin Boiarkin, Waqar Asif, Muttukrishnan Rajarajan, "Decentralized Demand Response Power Management System for Smart Grids" 2020 IEEE 8th International Conference on Smart Energy Grid Engineering (SEGE), ISSN:2575-2693.

[16] Jiarong Wu and Yimin Lu, "Adaptive backstepping sliding mode control for boost converter with constant power load", IEEE Access 12th April 2019; Volume:7:50797-50807.

[17] Ibrahim Yaichi, Harrouz Abdelkader, Boussaid Ibrahim, Abdel Hafid Semmah, Wira Patrice, Ilhami Colak, Korhan Kayisli, " An Improved DTC Strategy for a DFIG using an Artificial Neural Network Controller" 2021 IEEE 9th International Conference on Smart Grid (icSmartGrid), ISBN:978-1-6654-4531-3.

[18] Abdul Rehman Yasin, Amina Yasin, Mudassar Riaz, Muhammad Ehab and Ali Raza, "Filter extracted sliding mode approach for DC Microgrids", Electronics 2021, 10,1882: 1-12.

[19] M.Lakshmi and S.Hemamalini, "Non isolated high gain DC-DC converter for DC microgrids", IEEE Transactions on industrial electronics, Vol:65, Isuue: 2, Feb.2018: 1205-1212.

[20] Sadaqat Ali, Zhixue Zheng, Michel Aillerie, Jean-Paul Sawicki, Marie-Cecile Pera and Daaniel Hissel, " A review of DC Microgrid energy management systems dedicated to residential applications", Energies 2021, 14,4308: 1-26.

[21] Umar. T Salman, Mohammed A. Abdulgalil, Olaoti S. Wasiu, Muhammad Khalil, "Energy Management Strategy Considering Battery Efficiency for Grid-Tied Microgrids During Summer in the Kingdom of Saudi Arabia", 2019 IEEE 8th International Conference on Renewable Energy Research and Applications (ICRERA), ISSN:2572-6013.

[22] Hasan Erteza Gelani, Faizan Dastgeer, Kiran Siraj, Mashood Nasir, Kamran Ali Khan Niazi and Yongheng Yang, "Efficiency Comparision of AC and DC Distribution Networks for Modern Residential Localities", applied sciences.2019,9, 582.

[23] Tarek Boutabba, Said Drid and Larbi Chrifi-Alaoui, " Experimental control of photovoltaic system using neuro-Kalman filter maximum power point tracking (MPPT) technique", International Journal of Emerging Electric Power Systems 2020; 21(3).

[24] Ece Kurt, Gurkan Soykan, "Performance Analysis of DC Grid Connected PV System Under Irradiation and Temperature Variations", 2019 IEEE 8th International Conference on Renewable Energy Research and Applications (ICRERA), ISSN:2572-6013.

[25] Parusharamulu Buduma, Narendra Kumar Vulisi and Gayadhar Panda, " Robust control and kalman MPPT for grid assimilated wind energy conversion systems", IEEE Transactions on industry applications, Vol. 57, No.2, March/April 2021: 1274-1284.

[26] Subramanian Vasantharaj, Vairavasundaram Indraandhi, Vairavasundaram Subramaniyaswamy, Yuvaraja Teekaraman, Ramya Kuppusamy and Srete Nikolovski, "Efficient Control of DC Microgrid with Hybrid PV-Fuel Cell and Energy Storage Systems", Energies 2021, 14, 3234.

[27] Hossein Shahinzadeh; Srete Nikolovski; Jalal Moradi; Ramazan Bayindir, "A Resilience-Oriented Decision-Making Model for the Operation of Smart Microgrids Subject to Techno-Economic and Security Objectives", 2021 IEEE 9th International Conference on Smart Grid (icSmartGrid), ISBN:978-1-6654-4531-3.